TECHNICAL UNIVERSITY OF CLUJ-NAPOCA

ACTA TECHNICA NAPOCENSIS

Series: Applied Mathematics and Mechanics
Vol. 55, Issue IV, 2012

RESEARCH ON HOW TO CONTROL THE POROSITY OF THE MEDICAL IMPLANTS MADE BY SELECTIVE LASER MELTING TECHNOLOGY

Răzvan PACURAR, Ancuta PACURAR, Adrian Sever RADU

Abstract: ***The article presents a series of researches that were performed for the first time in Romania, in the field of customized medical implants made by using the Selective Laser Melting (SLM) technology. Several samples were manufactured from TiAl6Nb7 material on the MCP Realizer SLM 250 equipment at the Technical University of Cluj-Napoca. Theoretical and experimental methods for determining the porosity of the metallic samples are also presented within the article. The connection between the lens positions of the optical system from the SLM machine and the resulted porosity within the internal structure of the material has been analyzed by using the Scanning Electron Microscope (SEM) images and ImageJ software. The samples were tested at traction in order to determine how the porosity is influencing other important material characteristics, such as the fracture strength resistance and the elongation at break. Actually, at the end, as demonstrated, by using the optimum lens position of the SLM machine, the fracture strength resistance and the elongation of the material, will not be significantly influenced, as compared to the values of these characteristics specified by the producer of the TiAl6Nb7 material.***

Key words: *Additive Manufacturing, Selective Laser Melting, Customized Medical Implants, Titanium.*

1. INTRODUCTION

The machinability of the titanium and titanium-alloyed materials is one of the most important topics within the bio-medical industry, this type of materials being applied on a large scale of applications within the medical field [1],[2],[3]. Titanium material has good mechanical properties as compared to the other metallic materials, such as a proper elastic modulus and a proper fatigue strength resistance. The titanium material it is used within several medical applications due to the fact that it has a good oxidation rate in free air. Actually, the titanium dioxide establishes a good bivalent connection on the molecular level between the implant and the human bone tissue [4],[5],[6].

The Additive Manufacturing (AM) technologies are used in a large scale of applications within the bio-medical field and particularly, in the field of customized medical implants, that are made using these types of technologies. Selective Laser Sintering, Selective Laser Melting and Electron Beam Machining are only few of these technologies that are able to be used in the field of medical implants. The Selective Laser Melting technology differs from other mentioned technologies by the fact that allows the user to manufacture metallic parts with a quite high-density level. In some cases, there were reported results that sustain the fact that by using the SLM technology, it is possible to manufacture near full-dense metallic parts [7], [8]. The possibility to control the porosity of the material it is very important in the medical field due to the fact that if the porosity is quite high, this will help the human tissue to be integrated into the manufactured structure more easy than if the structure is a fully dense one [9],[10]. Meantime, the structure of the implant must be a solid one, in order to not affect its durability and mechanical characteristics, as well [11], [12].

There are a lot of advantages in using such technology for manufacturing the medical implants, starting with the complexity of the model, which is not an impediment for the SLM technology, the part being materialized layer by layer [13],[14]. The time needed in order to finish the complex part is obviously, very short in this case, too. The lost of material is insignificant [15]. In consequence, the Selective Laser Melting (SLM) technology was easily adopted within the medical field, due to these advantages mentioned above [16],[17].

2. POROSITY THEORETICAL APPROACH

A number of physical phenomena are possible for the formation of pores inside laser-melted metallic structures. Three types of pores can be identified in the material structure, as illustrated in Figure 1 and presented below:
- large interconnected pores outside the balls caused by balling phenomenon
- relatively smaller pores inside the balls
- remained pores in the metallic structure after the welding process

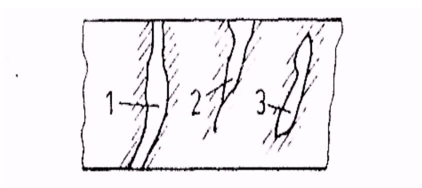

Fig. 1. Types of pores – outside the balls, inside the balls and remained pores

Powder material always contains a considerable amount of air inside it in between the particles. The non-uniform porosity distribution of the porous material surface has an important influence over its mechanical and technological characteristics.

From the theoretical point of view, the porosity of the material can be calculated very simple using the formula (1):

$$P = \frac{\Delta V}{V} * 100\,[\%] \qquad (1)$$

where:
P –porosity of the sample [%]
ΔV – pores volume within the structure of the sample [cm^3]
V – total volume of the sample, determined by using the law of Archimedes [cm^3]

As it could be observed from formula (1), the porosity P can be expressed as a report between the volume of pores ΔV and the total volume of the sample V.

The volume of the sample V can be determined by using formula (2)

$$\rho_r = \frac{m}{V}\,[\text{g/cm}^3]; V = \frac{m}{\rho_r}\,[\text{cm}^3] \qquad (2)$$

where:
m – mass of the sample (determined by using an analytic balance) (g)
ρ_r – real density of the sample [g/cm^3]

The volume of the pores within the sample's structure can be determined using formula (3):

$$\Delta V = V - Vo\,[\text{cm}^3] \qquad (3)$$

where:
V_0 – total volume of the sample, determined for the ideal case of the material

The total volume of the sample for the ideal case of the material, V_0 can be determined using formula (4):

$$\rho_0 = \frac{m}{V_0}\,[\text{g/cm}^3] \Rightarrow V_0 = \frac{m}{\rho_0}\,[\text{cm}^3] \qquad (4)$$

where:
ρ_0 – ideal density of the material (as specified by the metallic powder producer within the material's datasheet) [g/cm^3] – in the case of TiAl6Nb7 material, a value of 4,5 [g/cm^3] has been taken into consideration

As we can conclude by analyzing the formulas from (1) to (4) there is a close connection between the porosity of the material and its density. Actually these two characteristics are being considered as being complementary ones. If the density would be significantly increased, then the porosity of the material will be significantly decreased and vice-versa. The increase of porosity level into the material structure will have a significant consequence over the durability of the customized medical implant.

3. POROSITY EXPERIMENTAL APPROACH

3.1. Working principle of the SLM process

The working principle of the SLM process it is easy to be understood, as could be observed from the image illustrated in Figure 2.

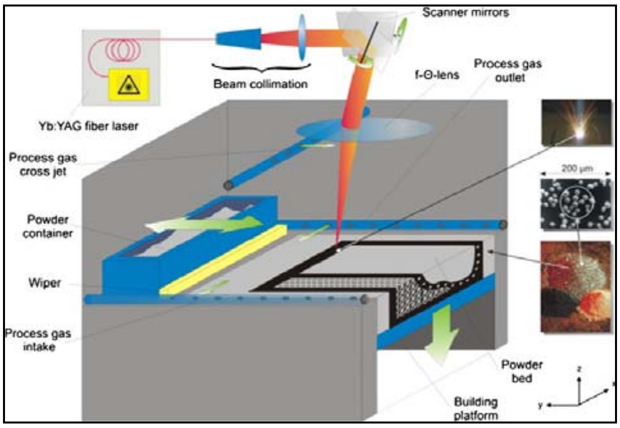

Fig. 2. Working principle of the SLM process

There are several steps that have to be fulfilled. Before starting the process, an inert gas (nitrogen or argon) will be introduced in the SLM machine chamber, through a circulating system as presented in Figure 2, until an inert atmosphere will be obtained inside the working chamber (the maximum level of oxygen admitted inside is 0,1 %). Further on, the inert gas will be circulated through the system during the entire process until the end, with a level of 0,1 % of oxygen maintained constant.

The process continues with the deposition of the raw material from the powder container over the building platform by using a wiper that it is moved along Y-axis direction.

The thickness of the deposed material is around 20-100 microns for the first few layers. The process is repeated until the powder covers the entire building platform uniformly. Then the layer thickness will be set to a constant value of 30 – 50 microns and the process continues with the scanning of the first layer according to the first slice of the model, and then will continue with the scanning of the next slice and so on until the part will be finished on the machine.

The scanning system of every layer (numerically controlled on X and Y-axes) it is composed by an ytterbium laser fiber source that emits a laser beam and the optical system composed by the scanning mirrors and lenses that are needed in order to focus the laser beam onto the building platform at the end (see Figure 3). The building platform it is moved on Z-axis direction, after the scanning process of every layer.

Finally, when the maximum height of the building packet is reached, the building platform will be moved reversed to the start position, and the manufactured packet will be removed from the platform after sucking the non-melted metallic powder and after eliminating the metallic supports that were generated within the control software of the SLM system, as well. The metallic supports have a wired structure and are obligatory needed in the manufacturing process in order to maintain the build part onto the manufacturing platform.

The tensions during the SLM process are very high, having the tendency of severely deforming the part during the manufacturing process, if it is not properly welded on the building platform starting with the first layers.

Besides the way of constructing and eliminating of the metallic supports on the post-processing stage, a very important issue is represented by the adjustment of the optical system of the SLM machine illustrated in Figure 3, so as the user will be working in the right focusing plane of the machine.

The calibration procedure is referring actually to the position adjustment of the focusing lens, in correlation with the X-Y scanning mirrors, so as the focus distance will be the optimum one at the end. If the focusing lens will be not in the right position, than the focus plane will be situated above or below the building platform plane.

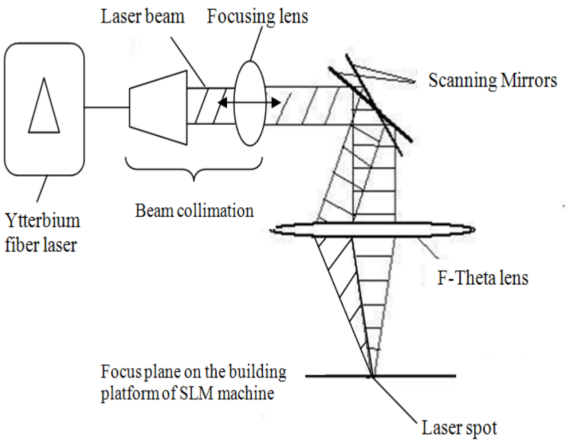

Fig. 3. The optical system of the SLM machine

This will have consequences over the manufactured part and its mechanical properties at the end, as it will be shown in the following chapters of the article. In this way, the porosity of the metallic structure can be controlled, if the lens position will be accordingly adjusted to the end.

3.2. Samples manufactured by SLM at the Technical University of Cluj-Napoca

In order to study the influence of the lens position technological parameter, over the porosity of the metallic parts made by SLM, 13 samples as the ones presented in Figure 4 were manufactured using the MCP Realizer II SLM 250 equipment from the Technical University of Cluj-Napoca illustrated in Figure 5.

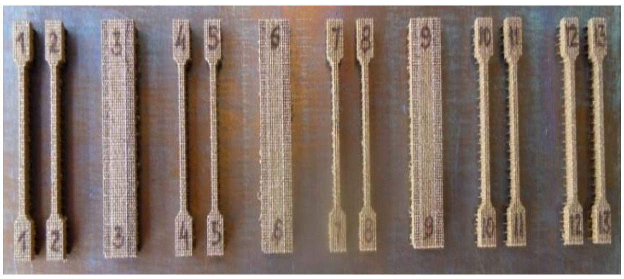

Fig. 4. A set of samples manufactured by SLM from TiAl6Nb7 material

The Lens Position Hatch Solid parameter and the Lens Position Fill Contour Solid parameter were differently varied in the case of 13 manufactured samples. This means that the hatching and filling contour was scanned on every case using different lens positions as compared to the starting position (the current position that was as the reference position set on the SLM machine).

Fig. 5. The MCP Realizer II SLM 250 machine from the Technical University of Cluj-Napoca

This will affect the internal structure of the material and the quality surface on the contour at the end, as well.

The main purpose of the experimental research was to determine the optimum lens position that leads to a proper welding and a compact state of the welded metallic granules.

Beside the lens position parameter, there were other important technological parameters that were used within the SLM manufacturing process, such as the scanning speed, the laser power, the hatching distance and the layer thickness.

The value of this technological parameters used in the manufacturing process of the samples are briefly presented in Table 1.

Table 1.
Technological parameters used within the SLM process of samples

Laser power [W]	Scanning speed [m/s]	Hatching distance (X&Y) [mm]	Layer thickness [µm]
200	0.4	0.12	50

3.3. Results and made calculus

In order to weight the samples and to determine the volume of the samples manufactured by SLM, the analytic balance and graduated cylinder, as the ones illustrated in Figure 6 were used.

Fig. 6. The analytic balance and graduated cylinder used to determine the mass and volume of the samples manufactured by SLM

The results of the made calculus using formula (1) to (4) are presented in detail in Table 2.

Table 2

The obtained results

Sample no.	m [g]	V [cm^3]	ρ_r [g/cm^3]	V_0 [cm^3]	ΔV [cm^3]	P [%]
1	21.872	2.9	4.24	2.73	0.17	6.07
2	21.261	2.92	4.10	2.66	0.26	9.88
3	20.867	2.9	4.05	2.61	0.29	11.19
4	20.568	2.84	4.16	2.57	0.21	8.13
5	20.779	2.82	4.27	2.60	0.14	5.50
6	21.225	2.82	4.23	2.65	0.17	6.29
7	21.749	3	4.08	2.72	0.28	10.35
8	21.695	2.86	4.27	2.72	0.16	5.46
9	21.397	2.86	4.21	2.67	0.19	6.93
10	22.142	2.9	4.29	2.77	0.13	4.78
11	22.012	2.86	4.33	2.75	0.11	3.94
12	21.957	2.78	4.44	2.74	0.04	1.29
13	21.903	2.78	4.43	2.74	0.04	1.54

As it is possible to observe from the results presented in Table 2, there is a maximum value of the porosity as calculated in the case of sample number 3 (the calculated porosity was 11,19 % , in this case). The minimum value of the porosity as calculated was 1,29 % , as it was determined in the case of sample number 12. This fact proves that there is a close connection that exists between the use of the SLM machine within the focus plane limit and the resulted porosity of the metallic part. If a metallic part that it is manufactured by SLM contains pores within the internal structure, this will severely influence its mechanical resistance, as well. Actually, if we make a difference between the maximum and minimum value of the porosity, this would be unacceptable - 9,9 %.

As related to the density variation presented in Table 2, there also can be observed that the maximum value of density was obtained as calculated in the case of sample number 12 (ρ=4.44 [g/cm^3]), as compared to a minimum value that has been obtained in the case of sample number 3 with a value of ρ=4.05[g/cm^3], as determined. This means that there is a close connection between the reducing of the pores fraction ratio within the internal structure of the material and the increasing of the material's density, as well.

Actually, the fracture strength will be decreased in this case, with a value of approximately 30 %, if we perform a calculus, according to formula (5).

$$Y = Y_s * 10^{-K_s * P} \qquad (5)$$

where: Y- is the fracture strength of the material with porosity P (%)

Y_s – is the fracture strength of the material for the ideal case – Y_s = 1185 N/mm^2 for the ideal case as specified by the TiAl6Nb7 material producer within the material datasheet.

P- is the porosity of the material (%)

K_s – is a constant coefficient that is dependent by the materials nature and the mechanical characteristic taken into consideration. In the case of titanium material, the coefficient K_s could take the following values: K_s = 0,049 in the case when the Hardness Brinell needs to be determined; K_s = 0,043, in the case when the fracture strength needs to be determined; K_s =0,058 in the case when the elongation of the material needs to be determined.

In our analyzed case, a factor K_s = 0,043 has been taken into consideration.

All manufactured samples were tested afterwards on the Galdabini equipment from the Technical University of Cluj-Napoca, in order to determine the material curve as illustrated in Figure 7.

The material properties we were interested in where the fracture strength and the material elongation.

The obtained results are presented in detail within Table 3. If we compare the obtained results with the characteristics presented by the materials producer in the material datasheet, there are not so big differences between the fracture strength resistance and the elongation of the material experimentally determined, as well.

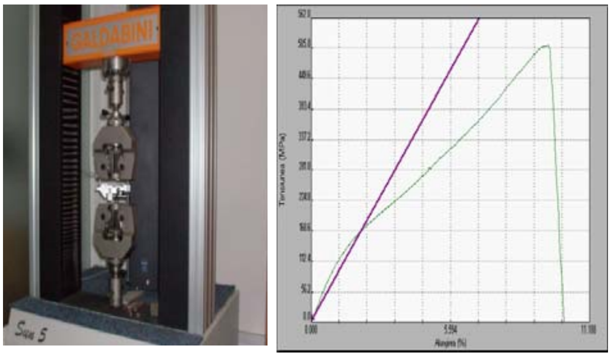

Fig. 7. Testing the SLM samples on the Galdabini equipment from TUCN

The specified value in the case of the ideal material is: for the Fracture strength - 1185 N/mm^2, and for the Elongation at break - 18 %. The maximum values we had experimentally determined were 1172.50 N/mm^2 for the fracture strength and 17.7 % in the case of sample number 12.

Table 3

Fracture strength and specific elongation of the samples manufactured by SLM

Samp. no.	F_{max} [N]	dL [mm]	S_0 [mm^2]	σ_r [N/mm^2]	ε_r [%]	l_0 [mm]
1	2880	9.3	4.1	1165.44	15.7	25
2	2832	9.4	4.24	1161.68	15.3	25
3	2762	9.2	4.32	1154.59	13.2	25
4	2910	11.9	4.78	1165.56	15.5	25
5	2890	10.2	4.4	1157.18	16.9	25
6	2745	9.5	4.61	1155.21	12.8	25
7	2820	9.4	4.41	1154.27	11.7	25
8	2920	12.1	4.51	1168.16	16.9	25
9	2795	9.6	4.4	1152.36	13.5	25
10	2825	10.5	4.51	1155.26	15.6	25
11	2780	9.7	4.2	1157.90	14.3	25
12	2970	10.3	4.4	1172.50	17.7	25
13	2710	9.5	4.1	1158.98	17.4	25
Mean value	2834	10.04	4.38	1159.93	15.1	25

The mean value of the fracture strength has been 1159.93 N/mm^2 for the fracture strength and 15.1 % for the elongation at break, which means that we had a difference of about 25 N/mm^2 in the case of fracture strength and a difference of about 2.9 % in the case of elongation at break, as compared to the ideal case, probably due to the remained pores inside the material structure.

Actually, the porosity of the material can be determined also by the experimental point of view, using the images taken from a scanning electron microscope (SEM).

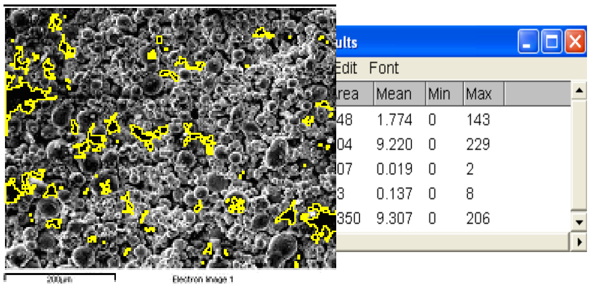

***Fig. 8.** ImageJ software analyzer*

ImageJ software was used to analyze the images. The porosity in this case was calculated by using the following formula:

$$p = \frac{\sum Ai}{Atot} \qquad (6)$$

where A_i represents each granule area and Atot is the entire image area.

As we could notice from the SEM images that were analyzed by using the ImageJ software, besides the internal defects that occurred in the case when the sample has been manufactured with a lens position adjusted outside the focus plane limit, the metallic granules were partially welded during the scanning process, too.

The density energy was also too high in this case. This had caused a lot of tenses within the internal structure of the material.

These tenses were severely increased, accordingly, as the SLM process went on. Meanwhile, when the sample has been manufactured with a lens position adjusted within the focus plane limit, we could notice the absence of the internal defects, such as cracks and pores. The sample number 12 corresponded by the internal structure point of view, as it has been determined also by ImageJ software analysis, so the lens position of the SLM machine was adjusted at the end with a value of +30 [μm] as compared to the starting position (the initial one that has been considered as the reference position).

The new value of the lens position that it was set on the MCP Realizer II SLM 250 machine at the Technical University of Cluj-Napoca has determined the manufacturing process to run within the focus plane limit of the machine.

4. CONCLUSIONS

In conclusion of our made research, we could state that the Selective Laser Melting technology it is easy to be understood in principle, but it is not so easy to be controlled.

The lens position has an important influence over the material structure of metallic parts made by SLM, as demonstrated by the Scanning Electron Microscope (SEM) analysis. From the set of samples that were manufactured using the SLM machine, the sample number 12 has corresponded by the internal structure point of view, so the lens position has been adjusted with a value of +30 [μm], as compared to the starting position.

As demonstrated, there is a close connection between the use of the Selective Laser Melting machine within the focus plane limit and the resulted mechanical properties of the metallic part, as well.

The reducing of the pores fraction ratio within the internal structure of the material and the increasing of the material's density, are, as demonstrated in direct connection, too. As determined, the highest density value was obtained in the case of sample number 12 (ρ=4.44 [g/cm^3]), as compared to the minimum value that has been obtained in the case of sample number 3 with a value of ρ=4.05[g/cm^3]. This is severely affecting the fracture strength resistance, as well. The fracture strength will be decreased in this case, with a value of approximately 30 %.

The experimental research that has been made on the MCP Realizer II SLM 250 machine, at the Technical University of Cluj-Napoca, using the adjusted lens position, confirmed that there were not so big differences between the fracture strength resistance and the elongation of the material, as compared to these characteristics values in the ideal case, as specified by the producer of the TiAl6Nb7 material.

The resulted differences of about 25 N/mm^2 in the case of the fracture strength and of about 2.9 % in the case of the elongation at break were caused mainly by the remained pores inside the material structure. The lowest porosity that has been obtained in the case of a metallic sample made by SLM was 1,29 %.

5. REFERENCES

[1] J. Emsley, *Nature's Building Blocks: An A-Z Guide to the Elements*, Oxford University Press, 2001, pp. 451 – 53.

[2] B. D. Boyan, F. F. Bonewald, E. P. Paschalis, C. H. Lohmann, J. Rosser, D. L. Cochran, D. D. Dean, Z. Schwartz, A. L. Boskey, *Osteoblast-mediated mineral deposition in culture is dependent on surface microtopography*, Calcif, Tissue Int. 2002, 71, 519-529.

[3] M. Benedetti, V. Fontanari, *The effect of bi-modal and lamellar microstructures of Ti-6Al-4V on the behaviour of fatigue cracks emanating from edge notches*, Fatigue and Fracture of Engineering Materials and Structures 2004, 27, 1073-1089.

[4] B. Feng, J. Y. Chen, S. K. Qi, L. He, J. Z. Zhao, X. D. Zhang, *Characterization of surface oxide films on titanium and bioactivity*, J. of Materials Science: Materials in Medicine 2002, 13(5), 457-464.

[5] L. C. Moreno, L. Garcia-Pineros, E. Delgado-Mejia, *Triple alkaline treatment of titanium surfaces for calcium phosphates growth*, Braz. J. Phys. 2006, 36, 3-7.

[6] K. Hamada, M. Kon, T. Hanawa, K. Yokoyama, Y. Miyamoto, K. Asaoka, *Hydrothermal modification of titanium surface in calcium solutions*, Biomaterials 2002, 23, 2265-2272.

[7] N. Sahai, M. Anseau, *Cyclic silicate active site and stereochemical match for apatite nucleation on pseudowollastonite bioceramic–bone interfaces*, Biomaterials 2005, 26(29), 5763-5770.

[8] S. Ban, *Effect of alkaline treatment of pure titanium and its alloys on the bonding strength of dental veneering resins*, J. Biomed. Mater. Res. A 2003, 66(1), 138-145.

[9] S. Ban, A. Kadokawa, T. Kanie, H. Arikawa, K. Fujii, T. Tanaka, *Bonding strength and durability of alkaline-treated titanium to veneering resin*, Dent. Mater.J. 2004, 23(3), 424-428.

[10] Y. Xie, X. Liu, A. Huang, C. Ding, K. P. Chu, *Improvement of surface bioactivity on titanium by water and hydrogen plasma immersion ion*

implantation, Biomaterials 2005, 26(31), 6129–6135.

[11] X. Liu, R. W. Y. Poon, S. C. H. Kwok, P. K. Chu, C. Ding, *Structure and properties of Ca-plasma-implanted titanium*, Surface and Coatings Technology 2005, 191, 43–48.

[12] B. Elmengaard, J. E. Bechtold, V. Soballe, *In vivo study of the effect of RGD treatment on bone ongrowth on press-fit titanium alloy implants*, Biomaterials 2005, 26 (17), 3521-3526.

[13] C. Popa, V. Simon, I. Vida-Simiti, G. Batin, V. Candea, S. Simon, *Titanium – Hydroxyapatite Porous Structures for Endosseous Applications*, Journal of Materials Science: Materials in Medicine 2005, 16, 1165-1171.

[14] L. G. Harris, R. G. Richards, *Staphylococcus aureus adhesion to different treated titanium surfaces*, Journal of Materials Science: Materials in Medicine 2004, 15(4), 311-313.

[15] L. G. Harris, L. Mead, E. Muller-Oberlander, R. G. Richards, *Bacteria and cell cytocompatibility studies on coated medical grade titanium surfaces*, J. Biomed. Mater. Res. 2006, 78(1), 50-58.

[16] B. O'Brien, W. M/ Carroll, M. J. Kelly, *Passivation of nitinol wire for vascular implants—A demonstration of the benefits.* Biomaterials 2002, 23, 1739–1748.

[17] B. C. Carr, and T. Goswami. *"Knee Implants – Review of Models and Biomechanics"*. Materials & Design, 30(2):398-413, 2009.

Cercetări privind controlul porozității implanturilor medicale personalizate fabricate prin metoda topirii selective cu laser

Rezumat: În lucrare se prezintă o serie de cercetări care au fost dezvoltate în premieră în România, în domeniul fabricării rapide a implanturilor medicale personalizate, utilizând tehnologia Topirii Selective cu Laser. O serie de epruvete au fost fabricate în cadrul Universității Tehnice din Cluj-Napoca dintr-un material pulverulent de tipul TiAl6Nb7, disponibil comercial pentru sistemul de fabricație MCP Realizer II SLM 250. Metodele teoretice şi experimentale utilizate în vederea determinării porozității acestor epruvete sunt prezentate de asemenea în detaliu în cadrul acestei lucrări. Epruvetele au fost testate la tracțiune în vederea determinării unor caracteristici importante de material, pentru a putea demonstra modul în care porozitatea influențează rezistența la rupere a acestor epruvete şi alungirea acestora. În finalul cercetărilor, s-a putut observa faptul că există o legătură strânsă între sistemul optic al echipamentului de topire selectivă cu laser, porozitatea rezultată în structura materialului şi celelalte caracteristici importante de material, cum sunt rezistența la rupere sau alungirea materialului.

Razvan Pacurar, Dr. Eng., Teaching Assistant, Technical University of Cluj-Napoca, Department of Manufacturing Engineering, B-dul Muncii, no.103-105, 400641, Cluj-Napoca, razvan.pacurar@tcm.utcluj.ro, 0040-264-401784.

Ancuta Pacurar, Dr. Eng., Teaching Assistant, Technical University of Cluj-Napoca, Department of Manufacturing Engineering, B-dul Muncii, no.103-105, 400641, Cluj-Napoca, ancuta.costea@tcm.utcluj.ro, 0040-264-401721.

Adrian Sever Radu, Dr. Eng., Teaching Assistant, Technical University of Cluj-Napoca, Department of Manufacturing Engineering, B-dul Muncii, no.103-105, 400641, Cluj-Napoca, adrian.radu@tcm.utcluj.ro, 0040-264-401784.